

Ancient harbours used as tsunami sediment traps – the case study of Krane (Cefalonia Island, Greece)

A. Vött¹, H. Hadler¹, T. Willershäuser¹, K. Ntageretzi¹, H. Brückner², H. Warnecke³, P.M. Grootes⁴, F. Lang⁵, O. Nelle⁴, D. Sakellariou⁶

¹ Institute for Geography, Johannes Gutenberg-Universität Mainz, Johann-Joachim-Becher-Weg 21, 55099 Mainz, Germany

² Institute for Geography, Universität zu Köln, Albertus-Magnus-Platz, 50923 Köln, Germany

³ In der Mulde 10, D-51503 Rösrath-Forsbach, Germany

⁴ Leibniz Laboratory for Radiometric Dating and Isotope Research, Christian-Albrechts-Universität zu Kiel, Max-Eyth-Str. 11-13, 24118 Kiel, Germany

⁵ Department of Classical Archaeology, Technische Universität Darmstadt, El-Lissitzky-Str. 1, 64287 Darmstadt, Germany

⁶ Hellenic Centre for Marine Research (HCMR), 47th km Athens-Sounio Ave, 19013 Anavyssos, Greece

Corresponding author: voett@uni-mainz.de

Abstract

Geoarchaeological studies in the environs of ancient Krane (Cefalonia Island) were conducted to reconstruct palaeoenvironmental changes and to identify the location of the ancient harbour. Altogether 9 vibracores were drilled at the (south-)eastern shores of the Bay of Koutavos and in the Koutavos coastal plain. Sediment cores were analyzed by means of sedimentological and geomorphological methods. A local geochronostratigraphy was achieved based on radiocarbon AMS dates and archaeological age estimations of diagnostic ceramic fragments. Earth resistivity measurements helped to detect subsurface structures and to correlate stratigraphies over long distances. The local stratigraphical record comprises signals of both an autochthonous gradual coastal development and repeated interferences related to high-energy events. As the Bay of Argostoli and Koutavos, due to its cul-de-sac-type topography, represents an excellent natural harbour completely sheltered from storm influence and as the wider region is well known to have experienced multiple tsunami impacts during history triggered by the adjacent Hellenic Arc, ex situ-marine depositional interferences are interpreted to be caused by multiple tsunami landfall. Geochronological data

yielded maximum ages for the tsunami event generations I to IV of 4150 ± 60 cal BC, $\sim 3200 \pm 110$ cal BC, $\sim 650 \pm 110$ cal BC, and $\sim 930 \pm 40$ cal AD, respectively. It remains speculative to infer from our geoarchaeological reconstructions that the development of the polis was crucially affected by tsunami impact because historical and archaeological data from ancient Krane are sparse. In contrast to Partsch (1890), we suggest the harbour of ancient Krane lying at the (south-)eastern shore of the Bay of Koutavos where perfect conditions in terms of water depth and access exist. Our study shows that ancient harbours such as the one of Krane represent excellent archives to detect the number, dimension, intensity and spatial extent of supra-regional tsunamis.

1. Introduction

Interdisciplinary research on ancient harbours in the eastern Mediterranean on the part of archaeological and geographical sciences has been strongly intensified during the past two decades. Nowadays, ancient harbours are mostly landlocked and may even lie many kilometers inland because coastlines have shifted dramatically since ancient times (Vött and Brückner 2006, Marriner and Morhange 2007, Marriner et al. 2010). An example for considerable coastline changes is Piraeus, site of the present-day harbour of Athens, which was an island until the midst of the 2nd millennium BC (Goiran et al. 2011) and is now part of the Attic mainland. The main objectives of geoarchaeological research in ancient harbour areas are to locate harbour basins as such and to clarify how they were connected to the sea. At Miletus, Priene and Myous (western Turkey), for example, Müllenhoff (2005) and Brückner et al. (2006) reconstructed the local palaeogeographical settings and identified several landing sites. In western Greece, the shipsheds of ancient Oiniadai were found to have been part of a lagoonal harbour whereas, on the other side of the former island, a potential river harbour was detected (Vött 2007, Vött et al. 2007). For Pella, northern Greece, Fouache et al. (2008) and Ghilardi et al. (2008) showed that at the time of Alexander the Great the site of Pella did not lie at the coast but at the shore of a large lake that was connected to the sea via a man-made channel. Complex geoarchaeological harbour studies were also conducted at Claudius and Trajan's marine harbours on the Tiber delta (Italy) with respect to access channels to the sea (Giraudi 2009, Goiran 2010). A further key question of harbour geoarchaeology is to reconstruct the time interval during which harbour facilities were in use and when and why they were abandoned. The palaeogeographical and paleoenvironmental settings of harbours were strongly altered in the course of time due to different factors such as sediment transport from the hinterland, changing coastal dynamics, sea level fluctuations and

man-made impact. In many cases, it is by these gradual changes that delta progradation and coastal aggradation were triggered and harbour installations experienced partial or complete siltation.

Within the past few years, however, strong evidence was found that ancient harbours were not only affected by gradual changes of the coastal environment but that they were also subject to strong event-related disturbance or destruction (Morhange and Marriner 2010). Reinhardt et al. (2006) and Goodman-Tchernov et al. (2009), for example, detected by underwater geoarchaeological studies that the harbour of Caesarea Maritima was destroyed by tsunami impact in 115 AD and that the site had already been affected by older tsunami impacts. For the harbour at Alexandria (Egypt), both sedimentological and microfaunal indicators of tsunami-related impact and destruction during the 365 AD earthquake and tsunami are well known (Stanley and Bernasconi 2006, Bernasconi et al. 2006). In 557 AD, the Byzantine harbour of Constantinople, Yenikapı, was completely erased by a strong tsunami (Bony et al. 2011). Manifold geo-scientific evidence of tsunami impact was also found for harbour sites in central and western Greece such as ancient Lefkada (Vött et al. 2009a, May et al. 2011) and Palairos-Pogonia (Vött et al. 2009b, 2011a). Recent studies have shown that the history of the Corinthian harbour at Lechaion, one of the most important ancient harbour sites in the Mediterranean, is related to repeated tsunami landfall that widely struck the eastern end of the Gulf of Corinth (Hadler et al. 2011). In the western Peloponnese, Olympia's harbour site Pheia was found to have been completely destroyed by co-seismic subsidence and coincidental tsunami rollover in the 6th century AD (Vött et al. 2011b).

By these studies, ancient harbours turned out to be excellent tsunami sediment traps. This is mostly due to the fact that harbours were constructed to protect ships and harbour facilities from storms but – by diffraction, refraction and amplification of waves caused by construction walls and piers – were highly prone to be affected by tsunami impacts, as is already indicated by the Japanese origin of the word itself (tsunami = harbour wave). Provided that by dredging activities, which were carried out to prevent the harbour basin from siltation, the stratigraphical record was not erased or completely altered, ancient harbour basins are thus perfect artificial tsunami sediment traps. Storm deposits are not expected to play a major role in the harbour sedimentary record, whereas tsunami sediments are widely present. The comparison of geostratigraphical data from coastal areas outside and inside ancient harbour settings allows distinguishing between the influence of tsunamis and storms on the coastal evolution – a question which is vividly debated in coastal geosciences all over the world. Identifying tsunami sediments, so called tsunamites, in ancient harbours is an emerging field

in modern geoarchaeological research as it combines aspects of man-environment interaction with the cultural and socio-economic background of harbour development and the geo-scientific quest to identify destructive tsunami events and their recurrence interval.

This paper focuses on the significance of the harbour of ancient Krane on Cefalonia Island (western Greece) as a tsunami sediment trap for deciphering the regional tsunami chronology. The main objectives of our geoarchaeological studies were (i) to detect the exact position of the ancient harbour in the environs of the Koutavos coastal plain, (ii) to reconstruct gradual palaeoenvironmental changes and their consequences for the site, and (iii) to find out the magnitude and frequency of tsunami impacts on the harbour since the mid-Holocene.

2. Natural settings and historical and archaeological background

Ancient Krane is located on top of a hill out of Cretaceous limestone some 60 to 110 m above present sea level (m a.s.l.) at the southeastern edge of the Bay of Koutavos (Fig. 1; IGME 1985). The Bay of Koutavos, approximately 1.5 km long and 900 m wide, is characterized by shallow water depths < 1 m, its length axis trending in SE-NW direction (Fig. 2). The sedimentary conditions are those of a shallow water quiescent lagoonal environment. During hot summer months high evaporation rates may cause anoxic conditions associated to the formation of hydrogen sulfide. Apart from a narrow drainage channel that brings freshwater from karstic springs at the foot of the Krane hill to the lagoonal shore, there are no apparent geomorphological signs of present fluvial activity in the Koutavos coastal plain.

High-resolution DGPS surveys conducted during the past two decades revealed that Cefalonia Island generally shows a net downward movement associated to the subduction of the African Plate underneath the Aegean Microplate along the Hellenic Arc which is located to the south of Cefalonia (Fig. 3; Clément et al. 2000). This movement, however, is episodically interrupted by relaxative co-seismic uplifts resulting in an overall yo-yo type movement of the crust (Hollenstein et al. 2008a, 2008b; see also Lagios et al. 2007). Straight offshore the western part of Cefalonia, the Hellenic Arc is represented by the Cefalonia Transform Fault (CTF) which leads over to a northerly adjacent zone of continent-continent collision (Sachpazi et al. 2000). The geotectonic constellation is known to provoke earthquakes like in 1953 when large parts of the island were destroyed and co-seismic uplift of up to 70 cm was observed at many coastal sites ($M = 7.2$, Stiros et al. 1994). The last major earthquakes occurred in 1983 on Cefalonia Island ($M = 7.0$, Scordilis et al. 1985) and in 2004 on the adjacent Lefkada Island ($M = 6.3$, Papadimitriou et al. 2006). Recent studies on Cefalonia have shown that both exposed coastal sections such as the Paliki Peninsula and inner parts of

the Gulf of Argostoli experienced repeated tsunami landfall, most probably triggered by local to regional earthquakes (Fig. 3; Vött et al. 2010, Willershäuser et al. 2011). Palaeo-tsunami signatures were also detected for the neighbouring Lefkada Island (Vött et al. 2009a) and coastal Akarnania (Vött et al. 2011a).

According to Partsch (1890) Mycenaean remains document early settlement activities along the shores of the Bay of Koutavos. Warnecke (2008) hypothesizes that Krane was the home town of Bronze Age Odysseus and that modern Cefalonia therefore corresponds to Ithaka in Homer's Iliad. Ancient Krane is already mentioned as polis by Thukydides (2.30.2) and seems to have fought aside the Athenian allies in the Corinthian aggression in 431/430 BC during the Peloponnesian War (Biedermann 1887, Gehrke and Wirbelauer 2004). Historic accounts do not give evidence of the existence of the polis far beyond 370 BC when Partsch (1890: 83f.) suggests that the city and its fortifications were abandoned unfinished due to an unknown catastrophe. The city and its acropolis are well fortified by polygonal and isodomic walls (Fig. 1) parts of which were erected to connect the hill with the adjacent Koutavos coastal plain. Partsch (1890: Table 2) postulates that the harbour of ancient Krane is situated at the northwestern tip of the coastal plain. However, this has not been verified so far.

3. Methods

First geoarchaeological investigations in the Koutavos coastal plain were conducted in 2003 under the auspices of the regional government (Nomarchia) of Cefalonia and the diocese of the island. Supplementary studies were carried out in 2010. Studies comprised vibracoring along the shores of the Koutavos coastal plain down to a maximum coring depth of 7 m below ground surface (m b.s.) using an engine-driven coring device type Cobra mk1 and core diameters ranging from 6 cm to 3.6 cm. Vibracores were cleaned, photographed and described in the field using geomorphological and sedimentological methods (Ad-hoc-Arbeitsgruppe Boden 2005). Macrofossil fragments were used to determine the sedimentary facies and to reconstruct palaeoenvironmental changes (Poppe and Goto 1991, 2000). Geochemical parameters analysed for selected sediment samples comprised pH-value, electrical conductivity, carbonate content, content of organic material (loss on ignition) and concentrations of (earth alkaline, alkaline and heavy) metals (Blume et al. 2011). Vibracore KOU 1A was recovered from site KRA 5 using sediment-filled plastic liners in 2010. In the laboratory, X-ray fluorescence measurements were conducted using a portable XRF spectrometer (type Niton X13t 900 GOLDD) to obtain total concentrations of around 30 elements. Earth resistivity measurements were carried out along two transects by means of a

multi-electrode geoelectrical instrument (Iris Instruments, type Syscal R1+ Switch 48) in order to screen subsurface conditions and to check for differences in the general stratigraphical sequence. Position and elevation of vibracoring sites and ERT transects were measured using a differential GPS (type Leica SR 530 and Topcon HiPer Pro). A geochronological frame was established by radiocarbon dating of selected organic samples or samples out of biogenically produced carbonate as well as by archaeological age determination of diagnostic ceramic fragments.

4. Geoarchaeological investigations in the Koutavos coastal plain

Within the framework of our geoarchaeological studies, we drilled 9 vibracores and analyzed 2 electrical resistivity transects (Figs. 1 and 4).

4.1 Vibracore stratigraphies

Vibracoring sites are located in the Koutavos coastal plain and at the southeastern (KRA 1 to 7), the southern (KRA 8) and the eastern shores of the Bay of Koutavos (KRA 9).

Vibracoring sites KRA 1 to 7 were arranged in the form of two more or less parallel SE-NW running transects (KRA 1, 2, 4, 3, 5; KRA 1, 2, 6, 7, 5) perpendicular to the present lagoonal shoreline (Fig. 4).

Vibracoring site KRA 1 (N 38°09'43.8", E 20°30'37.9", ground surface at 1.12 m a.s.l.) is located some 450 m inland. The lower part of the core (0.15 m below sea level (m b.s.l.) – 0.43 m a.s.l.) is made up of greyish brown, silty to clayey material enriched with grus and pebbles and including ceramic fragments, the grain size distribution being clearly bimodal and the sediment badly sorted. The upper part of the core is made up of brown clayey silt. At 1.27 m b.s. drilling was stopped by large blocks in the subground.

Vibracores KRA 2 to 7 (KRA 2: N 38°09'44.6", E 20°30'36.2", ground surface at 0.73 m a.s.l.; KRA 3: N 38°09'50.0", E 20°30'31.9", 0.58 m a.s.l.; KRA 4: N 38°9'47.2", E 20°30'32.6", 0.70 m a.s.l.; KRA 5/KOU 1A: N 38°09'56.9", E 20°30'29.3", 0.20 m a.s.l.; KRA 6: N 38°09'47.5", E 20°30' 30.9", 0.68 m a.s.l.; KRA 7: N 38°09'48.8", E 20°30' 28.4", 0.48 m a.s.l.) show an overall consistent stratigraphical pattern starting with reddish brown (bottom) to yellowish brown (top) clay-dominated deposits including only little carbonate or locally no carbonate at all. Due to the high iron content and the decalcified character, this facies is interpreted as a palaeosol, most probably late Pleistocene to early Holocene in age. On top, we found a homogeneous sequence of stiff grey deposits reaching from silty clay to clayey silt. In core KRA 7, this unit is almost 2 m thick (Fig. 5; 5.68-3.79 m b.s.l.). Due to its

moderate carbonate content and the fact that marine macrofaunal remains are missing, we assume deposition of the material in a shallow water limnic environment. However, at vibracoring site KRA 5, remains of a brackish fauna documents a lagoonal character of this unit. Towards the flank of Krane hill, at coring site KRA 3, the corresponding facies is a transition between limnic and fluvial, the alluvial input remaining fine-grained but brownish in colour. Towards the top of the cores, fine-grained sediments still prevail but become rust-coloured. Most striking, however, is that these deposits are repeatedly intersected by layers of unsorted sand, shell debris, pebbles, stones and ceramic fragments. Though the material of the intersecting layers appears coarse-grained and is mostly unsorted, it locally shows layering and includes rip-up clasts out of grey clay or silt originating from the underlying limnic deposits. In every case, the coarse-grained sediments follow on top of a sharp erosional unconformity. In several cores, their internal structure reveals multiple fining-upward sequences mostly starting with marine shell debris at the base, followed by a mixture of sand and ending with sandy silt at the top (Fig. 6). These features can be seen best in core KRA 7 which is illustrated in Fig. 5. Grain size and sedimentary characteristics of the intersecting deposits document that they were associated to an energetic level way higher than the one required for accumulating the fine-grained limnic sediments encountered below. By the occurrence of macrofaunal remains of marine origin, it is clear that the high-energy influence must have come from the seaside triggering the deposition of allochthonous material in an originally low-energetic environment. Each time after a high-energy impulse occurred, low-energy conditions were re-established and allochthonous sediments were subsequently covered by fine-grained clayey to silty deposits. Post-depositional rust-coloured staining of both allochthonous and overlying autochthonous deposits must be associated to an abrupt lowering of the groundwater level so that oxidation could start. We assume that this abrupt change of the groundwater level is caused by co-seismic uplift of coastal sections, a phenomenon which is well-known to have happened during recent earthquakes at Cefalonia (Section 2). Thus, cores KRA 2 to 7 do not only give sedimentary evidence of abrupt high-energy wave impulses but also of earthquakes as potential causative triggers of these events. Fig. 6 shows that, altogether, we found four different high-energy layers between the present lagoonal shore (KRA 5/KOU 1A) and up to 220 m inland (KRA 3, 7) and three high-energy layers up to 420 m inland (KRA 2, 4, 6). The most landward core KRA 1, some 460 m distant from the recent shore, still revealed one generation of high-energy deposits. High-energy deposits at the different coring sites were encountered in stratigraphically consistent positions. Fig. 6 depicts a general thinning inland tendency of the allochthonous high-energy layers

together with increasing elevations towards inland. With regard to thickness, composition and sedimentary characteristics, however, high-energy deposits revealed a considerable variability over short distances. The uppermost parts of the cores are made up of alluvial deposits, partly covered with rubble infill from the 1953 earthquake that destroyed the city of Argostoli almost completely (Moschopoulos and Marabegia-Kosta 2007).

In contrast to the stratigraphies found for the central shore and the Koutavos coastal plain, vibracore KRA 8 (N 38°09'51.7", E 20°30'05.5", ground surface at 1.45 m a.s.l.) – drilled some 65 m inland from the southern shore – revealed thick yellowish brown, clayey to silty alluvial deposits accumulated on top of the ubiquitous palaeosol unit (Fig. 7). However, the upper part of the core shows an intriguing intersecting layer (0.69-0.07 m b.s.l.) out of marine shell debris, sand and small pebbles with an erosional unconformity at the base and a sharp boundary towards the subsequently overlying fine-grained deposits. The material is partly cemented and resembles beachrock. From its sedimentary structure and composition and with regard to the clearly low-energetic in-situ conditions, this layer is a high-energy deposit par excellence (Figs. 7 and 9).

Vibracore KRA 9 (N 38°10' 20.2", E 20° 30' 27.3", ground surface at 0.09 m a.s.l.) was drilled some 700 m to the north of site KRA 5 at the eastern shore of the Bay of Koutavos. Here, the hill slope is steep and obviously bound to a SE-NW running fault system (IGME 1985). The overall predominant material is homogeneously grey clayey silt including macrofaunal remains of a brackish fauna thus mirroring a typical lagoonal environment (Fig. 8). However, similar to vibracores KRA 2 to 7, we found three distinct intersecting layers (6.51-6.04, 4.78-4.36, 2.66-2.06 m b.s.l.) of mostly marine shell debris, sand and individual pebbles and stones (Fig. 9). Associated sedimentological features such as erosional unconformities, distinct layering and incorporated rip-up clasts of eroded lagoonal deposits were also encountered. The uppermost coarse-grained layer (1.26 m b.s.l. – 0.01 m a.s.l.) is reported to have been dumped by the inhabitants of Argostoli after the earthquake that shook the island in 1953. Vibracoring site KRA 9 clearly documents a threefold high-energy impact that hit the Lagoon of Koutavos during the Holocene. Stratigraphical position and composition of the KRA 9 high-energy deposits are consistent with those found in the central Koutavos coastal plain (Fig. 9).

4.2 Earth resistivity measurements

We carried out two earth resistivity transects near vibracoring site KRA 5/KOU 1A. Transect KOU ERT 1 runs along, transect KOU ERT 2 perpendicular to the shore of the Bay of

Koutavos (Fig. 10). The area is characterized by massive building rubble, up to 2 m thick, that was dumped in the original coastal swamp during the 1990s as a land reclamation measure. According to the inverse model resistivity section of transect KOU ERT 1 the subsurface can be subdivided into two main units. Unit 1 lies below approximately 3 m b.s.l. and shows comparatively low resistivity values ($< 50 \Omega\text{m}$). On the contrary, unit 2 reaches resistivity values higher than $1000 \Omega\text{m}$. Compared to the stratigraphy of vibracore KRA 5, unit 1 corresponds to fine-grained autochthonous lagoonal deposits, whereas unit 2 clearly reflects overlying anthropogenic infill. Transect KOU ERT 2 has a higher vertical resolution which allows to better understand the transition between units 1 and 2. Fig. 10 illustrates that at the seaward end of the transect, units 1 and 2 are separated from each other by an intermediary unit with values between approximately 5 and $50 \Omega\text{m}$. This zone may correspond to the stratigraphical section of core KRA 5 that revealed multiple input of coarse-grained allochthonous material. Fig. 10 documents that the intermediary unit shows a landward decrease in thickness. Vibracoring site KRA 5 itself is not covered by building rubble as it is located at the mouth of a narrow drainage canal (see Section 2).

4.3 Geochemical analyses

In this paper, we present selected results of detailed geochemical analyses carried out for selected samples taken from vibracores KRA 1 to 9 and KOU 1A. Total concentrations of Ca and Ti, together with 28 other elements, were measured using a portable XRF analyzer (Type Thermo Niton Xl3t 900S) yielding laboratory quality data consistent with standard or specific calibrations, with results from laboratory XRF instruments, and with elemental concentrations measured in acidic solutions (Zhu and Weindorf 2010). Measurements were conducted using the SOIL software mode of the instrument. Each sample was continuously measured for 30 seconds using three different filters to obtain mean relative concentrations per measured element. The limit of detection for Ti concentrations is given as 0.01 ppm. For standardization issues and in order to eliminate potential influences of grain size and moisture, elemental ratios are preferred against absolute concentrations yielded per element. Elements were measured with a vertical resolution between several centimeters to decimeters per core depending on relevant changes in the stratigraphic record and sampling density.

With respect to the identification of allochthonous sediment layers in near-coast sedimentary archives, the Ca/Ti ratio of sediment samples is of special interest. Hereby, Ca is used as an indicator for marine influence as it is mainly brought into the elemental budget by carbonate shells of marine macro- and microfauna. On the contrary, Ti is produced through terrestrial

weathering of minerals such as feldspar, quartz and mica and by residual accumulation in limestone areas. The Ca/Ti ratio is thus an indicator for the relation between marine and terrigenous processes and their influences on geo-ecosystems. On a longer term, a general geochemical equilibrium is to be expected for every ecosystem unit. In contrast, high-energy impacts affect coastal ecosystems abruptly and temporarily so that they should leave unusual geochemical signals of restricted duration beyond the normal background. A similar methodological approach has already been approved within the framework of other studies dealing with the detection of tsunamites in ancient Greek harbours (Vött et al. 2011a, 2011b). However, potential post-depositional alteration of the carbonate content by subaerial weathering has to be taken into consideration. In the case of Krane, allochthonous high-energy sediments were deposited in a wet environment, and local decalcification, for instance induced by co-seismic uplift, remains secondary.

Fig. 11 shows a compilation of vertical Ca/Ti ratios obtained for vibracores KRA 2 to 9 and KOU 1A. In a general view, the Ca/Ti ratio is continuously increasing from the base towards the top of each profile. However, there are significant peaks that exceed the usual background trend by far. Comparing these Ca/Ti peaks with the overall stratigraphical pattern (Fig. 11) shows that each peak corresponds with a layer of allochthonous coarse-grained high-energy sediments. For vibracore KOU 1A, for example, we found four and for vibracore KRA 9 three distinct peaks representing clear interferences of the autochthonous system and being consistent with the stratigraphical data. Regarding vibracore KRA 8, the abrupt and temporary input of marine deposits into a terrestrial environment (1.52-2.14 m b.s.) is reflected by an outstanding Ca/Ti peak. Relatively high Ca/Ti values at the base of core KRA 3 correspond to an older palaeosol section that is weathered to a slightly lesser extent. Increased Ca/Ti values right below ground surface were found in areas where building rubble, rich in carbonate, was dumped.

4.4 Geochronostratigraphy of environmental changes

Altogether 9 samples out of organic material or biogenically produced carbonate were selected for ^{14}C -AMS dating (Table 1). As the variability in space and time of the marine reservoir effect for samples out of marine carbonate is still unknown, a mean marine reservoir effect of 400 years was assumed (Reimer and McCormac 2002). Diagnostic ceramic fragments encountered in sediment cores were used for cross-checking radiometric ages. Both radiometric ages and archaeological age estimates were considered within the stratigraphical

context in order to establish a geochronostratigraphy of high-energy events that struck the Bay of Koutavos (Figs. 6 and 9).

Dating high-energy events is a difficult task to fulfill due to several problems caused by complex erosional and depositional processes. This is especially true for processes associated to tsunami landfall. First, dating samples taken from the allochthonous high-energy deposit only yield maximum ages or *termini ad* or *post quos* for the event. The reason is that the event deposits might include reworked older deposits, which has been observed in many other case studies dealing with the reconstruction of palaeo-events (for example Vött et al. 2011b).

Second, the deposition of event sediments may be preceded by considerable erosion of the youngest pre-event deposits as indicated by the presence of ripped up sediment clasts out of underlying older material within the event layer. The dimension of the erosional hiatus produced by the event is impossible to estimate using radiocarbon and/or ceramic age dating; determining sedimentary ages for allochthonous high-energy deposits using the Optically Stimulated Luminescence (OSL) technique is the best theoretical option but practically problematic due to the high contents of carbonate in Mediterranean deposits. Carbonate crystals, other than quartz or feldspar, are not datable by the OSL method. Moreover, bleaching processes during the deposition of event layers turned out to be incomplete in some cases (for example Vött et al. 2011a). Third, dating of post-event sediments overlying the high-energy deposit is difficult in cases when the event deposits were accumulated in terrestrial environments above sea level where subaerial weathering is dominating. *Termini ante quos* for the event derived from post-event deposits are much closer to the date of the event if the deposits were brought into lagoonal or limnic environments where autochthonous sediment deposition is immediately re-established. At present, the so called sandwich dating approach is the most promising method to achieve a best-fit age interval for an event by dating both the underlying and the overlying deposits of an event layer. This kind of time bracketing yields a time window framed by a *terminus ad* or *post quem* below and a *terminus ante quem* above the event deposit. For example, radiocarbon sandwich dating helped to identify the first field evidence of the 365 AD Crete tsunamite in northwestern Greece in the Lake Voulkaria near Preveza (Vött et al. 2009b).

However, for the Krane case study, no datable material was found above or below the encountered event deposits. All ages given in Table 1 are thus mere maximum ages or *termini ad* or *post quos* for high-energy events that hit the Koutavos coastal plain. Samples KRA 7/7 M (4892-4776 cal BC) and KRA 7/6 HK (752-538 cal BC) originate from the same high-energy layer so that sample KRA 7/7 M has to be considered as reworked. The same is true

for sample KRA 9/8+ M (1122-996 cal BC) which was found associated to a ceramic fragment dating to the 16th-20th centuries AD. Finally, sample KRA 3/9 M yielded an age of 5043-4924 cal BC which considerably differs from the age of a ceramic fragment encountered in the same event layer dated to Roman to Byzantine times. This radiocarbon age is thus not considered reliable.

5. Discussion

5.1 The Bay of Koutavos – a tsunami sediment trap par excellence

The Ionian Islands are characterized by prevailing wind and wind-generated waves from western and northwestern directions (Hofrichter 2002, Soukissian et al. 2008). Maximum observed storm wave heights in the open Ionian Sea are not higher than 6-7 m (Scicchitano et al. 2007; Soukissian et al. 2007; De Martini et al. 2010). For areas some kilometers distant from the coast, the winter mean significant wave height is lower than 1.2 m and the probability of a significant wave event with a wave height > 4 m is almost nil (Medatlas Group 2004, Cavaleri 2005). On the base of gauge records, Tsimplis and Shaw 2010 show that seasonal sea level extremes are restricted to autumn and winter months and are less than 40 cm.

The shallow water lagoonal environment of the Bay of Koutavos together with the directly adjacent Bay of Argostoli follow the same SE-NW strike direction with water depths rapidly increasing from < 1 m to 26 m below present sea level (m b.s.l.) towards the NW (Fig. 2). With regard to the local topography and coastline configuration, they represent a cul de sac-type annex of the N-S running Gulf of Argostoli and are well protected from storms. The Bay of Argostoli and especially the Bay of Koutavos are completely sealed off from open sea wave dynamics. They represent one of the best storm-protected natural harbours in the Mediterranean. Today, Argostoli is one of the most important landing sites for large cargo, military and passenger ships on the Ionian Islands. The Gulf of Argostoli – more than 13.5 km long and 3.5 km wide – is, however, prone towards occasional storms from southern directions because of the comparatively long local fetch and channeling effects between the Cape of Aghios Theodoron and the coast at Lixouri (Fig. 2). Against this background, storms can definitely be excluded as being responsible for the deposition of high-energy event deposits encountered at the southeastern fringe of the Bay of Koutavos.

On the contrary, the Gulf of Argostoli is directly exposed towards the Hellenic Arc which is well-known to have triggered numerous tsunamigenic earthquakes in the past related to the subduction of the African Plate underneath the Aegean Microplate (see, for example,

Papazachos and Dimitriou 1991; Fig. 3). In case of a tsunami generated in the eastern Ionian Sea travelling towards a northern direction, the funnel-shaped coastline configuration between Argostoli airport and Cape Aghios Theodoron is supposed to enhance both tsunami wave height and tsunami velocity (Fig. 12) and trigger the following tsunami landfall scenario. The narrow and long middle and northern parts of the Gulf of Argostoli are expected to add a further acceleration momentum to the tsunami by channeling effects. Reaching Cape Aghios Theodoron, parts of the tsunami water masses are diverted to the SE into the Bays of Argostoli and Koutavos by wave diffraction. However, major parts continue travelling towards the northern end of the gulf where the high mountain ridges flanking the Livadi coastal plain reflect tsunami waters back southward. On their way back south, the promontory between Cape Aghios Theodorou and Argostoli acts as separating funnel branching off considerable tsunami water masses into the Bays of Argostoli and Koutavos. There, by their high velocity and inertia and through the quasi-continuous water inflow due to the long tsunami wave length, the tsunami waters reach the southeastern end of the cul-de-sac type embayment near Krane (Fig. 12). Subsequently, the water is reflected and drains off towards the NW back into the Gulf of Argostoli and the Ionian Sea.

The stratigraphical record encountered around ancient Krane documents multiple high-energy impact associated to both erosion of pre-existing fine-grained autochthonous and deposition of allochthonous coarse-grained sediments (Figs. 6 and 9; Section 4). According to the macrofossil content and geochemical fingerprints, the *ex situ*-material was transported to the Koutavos coastal plain from the seaside. As storms are not able to reach the study area let alone to leave significant imprints on the stratigraphical record, the tsunami scenario is the only plausible setting by which the occurrence, thickness, distribution and composition of allochthonous high-energy sediments can be explained. Based on the presented tsunami wave propagation scenario and field evidence by vibracoring, the Bay of Koutavos and the adjacent coastal plain are regarded as a (palaeo-)tsunami sediment trap par excellence.

5.2 Location of the harbour of ancient Krane

Partsch (1890), on the base of detailed field observations, supposed that the harbour of ancient Krane is located at the southwestern foot of Krane hill not far from the present shore of the Bay of Koutavos (Fig. 1). Our results from vibracoring, however, indicate that this area is not appropriate as a harbour site. Vibracores 3, 4, 6 and 7 mostly revealed thick sections of tsunami deposits while autochthonous lagoonal or limnic sediments hardly exceed 40-50 cm (Fig. 2). Even if parts of these deposits were eroded by tsunamigenic impact, the

corresponding water depth was not sufficient to allow navigating with larger ships. At the southern fringe of the bay near coring site KRA 8, no deposits belonging to a quiescent water body were discovered at all. On the contrary, vibracoring sites KRA 5 and especially KRA 9 lying at the immediate waterfront revealed thick lagoonal sequences that offered perfect conditions for anchoring (Figs. 8 and 9). We therefore suggest that the harbour installations of ancient Krane were most likely located right between sites KRA 5 and 9 where parts of the fortification system run towards the shore and nowadays lies an industrial area. This site would also be in favour of a short and rapid access to the western part of the ancient city.

5.3 Local event geochronostratigraphy

Results of ^{14}C -AMS dating and ages of diagnostic ceramic fragments are depicted in Figures 6 and 9 within the stratigraphical context. Vibracoring sites KRA 5 and 7 are considered as key sites for the area showing traces of four different tsunami generations. The oldest tsunami generation I obviously hit a pre-existing shallow water limnic environment whereas conditions had already turned brackish (lagoon) when generations II and III affected the area. Sedimentary traces of the youngest tsunami generation IV were only found at sites KRA 5 and 7 intersecting coastal swamp deposits. Radiocarbon ages obtained for samples from cores KRA 3, 5, 6, 7 and 9 represent mere maximum ages (Section 4.4).

Samples KRA 5/9+ M and KRA 9/15+ M are *termini ad* or *post quos* for tsunami generation I of 4351-4272 cal BC and 4210-4084 cal BC, respectively (Table 1). As they belong to the same stratigraphical unit, the younger age of 4210-4084 cal BC from sample KRA 9/15+ M is considered more reliable so that the maximum age of tsunami generation I is assumed as approximately 4150 ± 60 cal BC.

Stratigraphical comparisons between cores KRA 5, 7 and 9 show that sample KRA 7/11+ (4971-4855 cal BC) belongs to tsunami generation II; its age thus indicates strong reworking of older deposits. For tsunami generation II, only sample KRA 6/13 HK gives reliable age information. It yields a maximum age of 3326-3096 cal BC which is generally approved by a ceramic fragment from the same event layer that is probably as old as prehistoric times (Fig. 6).

Tsunami generation III is dated by sample KRA 7/6 HK to the time around 752-538 cal BC or later (Table 1). For tsunami generation IV, sample KRA 7/4 HK yielded an age of 894-969 cal AD or younger. Unfortunately, the ceramic fragments encountered in our vibracores were always related to high-energy event deposits. Thus, ages derived from diagnostic ceramic

fragments are also to be regarded as mere maximum ages and do not allow to refine the geochronostratigraphy based on radiocarbon datings.

5.4 Regional tsunami signals

During the past years, palaeotsunami studies have been intensified along the coasts of western Greece. With regard to tsunami generation I encountered in the Koutavos coastal plain and dated to approximately 4150 ± 150 cal BC or younger (Figs. 6 and 9), there are potentially correlating tsunamites published for the Bays of Palairos-Pogonia (Akarnania) and Aghios Andreas (western Peloponnese). A tsunami layer found in the central Palairos coastal plain yielded maximum ages of 4449-4360 cal BC and 4461-4356 cal BC (Vött et al. 2011a). A tsunamite described from ancient Pheia, harbour of Olympia, was radiocarbon dated using the sandwich approach to 4300 ± 200 cal BC (Vött et al. 2011b). These ages are in good accordance with the results from Krane and suggest a potential supra-regional tsunami event that hit Cefalonia, the western Peloponnese and coastal Akarnania in the last third of the 5th millennium BC.

Tsunamite generation II from Krane shows a maximum age of 3326-3096 cal BC which corresponds to a tsunamite maximum age found for the Palairos coastal plain of 3584-3414 cal BC (Vött et al. 2011a). This event is possibly identical with a supra-regional mega-tsunami that was dated to approximately 2900 cal BC and traces of which were found in the Sound of Lefkada (Vött et al. 2009a) and the Gulf of Corinth (Kortekaas et al. 2011). High-energy sediments of the same age that are associated to sedimentary features and a foraminiferal content indicating strong tsunami influence are also known from the Messenian Gulf (core AKO 1, southwestern Peloponnese, Engel et al. 2009).

Tsunamite generation III encountered near ancient Krane shows a maximum age of 752-538 cal BC (Table 1). It remains speculative if this event induced the abandonment of the polis in the 4th century BC (Section 2). Alternatively, it may be identical with or related to an event around 760 cal BC which struck the harbour at Lechaion of ancient Corinth (Hadler et al. 2011) and/or to one of several events (E9, E8, E7) between 800-400 cal BC documented by tsunami deposits identified in the Augusta Bay (eastern Sicily, De Martini et al. 2010, Smedile et al. 2011). In this case, event II would also represent a mega-tsunami of supra-regional nature.

Tsunami generation IV affected the Koutavos area at 894-969 cal AD or later. Smedile et al. (2011) identified tsunami impact for Augusta Bay (Sicily) for the time around 930-1170 cal AD (E3). Another potentially associated tsunami candidate from the 12th century AD found in

Siracusa (Sicily) is described by Scicchitano et al. (2010). Vött et al. (2006) report on geomorphological and sedimentological traces of a tsunami that struck the Bay of Aghios Nikolaos near Preveza between 1000 and 1400 cal AD. Tsunamigenic inundation of the Sound of Lefkada is reconstructed for the time during or after 1244-1293 cal AD (Vött et al. 2009a). Based on field evidence, Kortekaas et al. (2011) suggest that the Gulf of Corinth was affected by the 1402 AD tsunami. There is further sedimentary evidence that the southern Peloponnese was hit by tsunami impact around 1300 cal AD (Scheffers et al. 2008). Hence, it cannot be excluded that Krane tsunamite IV also has a supra-regional background. The time period of tsunami generation IV, other than tsunami generations I to III, is well known from catalogues to have experienced numerous catastrophic tsunami events (for example Guidoboni and Comastri 2005, Ambraseys 2009).

Although dating of the Krane tsunamites turned out to be difficult due the fact that only maximum ages are available (Figs. 6 and 9), our results document that the Koutavos coastal plain is an excellent tsunami sediment trap in which supra-regional tsunami signals seem to be widely recorded.

6. Conclusions

The Koutavos coastal plain (Cefalonia Island, western Greece) and the shores of the Bay of Koutavos were subject to geoarchaeological and geomorphological investigations aiming to detect the location of the harbour of ancient Krane as well as to determine gradual and event-related coastal changes. Stratigraphical data based on vibracores and earth resistivity measurements and geochemical data based on the analysis of sediment samples allowed to reconstruct palaeoenvironmental changes in space and time. ^{14}C -AMS dating helped to establish a geochronological time frame. Based on our results, the following conclusions can be made.

(i) The stratigraphical record of the Koutavos area revealed two different types of sediment. Besides fine-grained silt-dominated deposits accumulated in a shallow water or distal alluvial fan environment of a low energetic level, we found intersecting layers out of coarse-grained, sandy to gravelly material of marine origin rich in marine shell debris. The latter is associated to sedimentary characteristics typical of high-energy impact such as fining upward sequences, incorporated rip-up clasts and sharp erosional unconformities at the base (Figs. 5 to 9) with an overall thinning landward tendency of tsunami layers (Fig. 10).

(ii) Due to their cul-de-sac-type configuration as annex of the long and narrow Gulf of Argostoli, the Bays of Argostoli and Koutavos represent an excellent natural harbour belonging to the best storm-protected landing sites all over the Mediterranean (Fig. 2).

(iii) The Gulf of Argostoli is directly exposed to the seismically highly active Hellenic Arc which is, by historic accounts and well documented geo-scientific evidence, known to have triggered numerous tsunami events during the past millennia (Fig. 3). A tsunami inundation scenario (Fig. 12) based on the northward propagation of a tsunami into the Gulf of Argostoli plausibly shows that, by refraction, diffraction and reflection, considerable parts of the tsunami wave would reach the Bays of Argostoli and Koutavos and affect the Koutavos coastal plain.

(iv) Against the background of the natural storm-protected setting and the high tsunamigenic potential of the Hellenic Arc, we conclude that multiple allochthonous coarse-grained high-energy intersections encountered in the Koutavos coastal plain sedimentary archive were deposited by tsunami impact. The local stratigraphical record revealed four distinct tsunami layers related to four different tsunami generations (Figs. 6 and 9).

(v) Based on ^{14}C -AMS datings of organic samples and biogenically produced carbonate and archaeological age estimates of diagnostic ceramic fragments, maximum ages (*termini ad* or *post quos*) for the four encountered tsunami generations were found (I: $\sim 4150 \pm 60$ cal BC; II: $\sim 3200 \pm 110$ cal BC; III: $\sim 650 \pm 110$ cal BC; IV: $\sim 930 \pm 40$ cal AD; Figs. 6 and 9, Table 1). By comparison to palaeotsunami impacts known and dated for the wider region, it is suggested that Krane tsunami generations I to IV reflect tsunami impacts that affected the Ionian Islands, the Peloponnese and the coasts of the western central Greek mainland. The Koutavos coastal area thus seems to be an excellent archive for tsunami events of a supra-regional nature.

(vi) The autochthonous palaeogeographical evolution of the Koutavos coastal plain starts with a late Pleistocene to early Holocene palaeosol which is subsequently covered by lacustrine deposits of a shallow freshwater lake. Initiated by tsunamigenic impact, the water body then became brackish but still remained shallow (Figs. 5 to 9). After having experience repeated tsunami landfalls the lagoon was finally silted up by alluvial and colluvial deposits. Our data show that the Koutavos coastal plain was not an appropriate location for the harbour of ancient Krane (Partsch 1890). On the contrary, the central (south-)eastern shores of the Bay of Koutavos revealed excellent conditions for harbour installations such as a sufficient water depth and direct connection to the polis (Figs. 8 and 9). We therefore conclude that the Koutavos lagoon as such was used as harbour during antiquity.

(vii) Geoarchaeological studies in the vicinity of ancient Krane revealed that ancient harbours represent outstanding archives to detect the number, dimension, intensity and spatial extent of tsunamigenic impacts. Using ancient harbours as palaeotsunami archives, a (supra-)regional tsunami chronology can be established. Palaeotsunami research in ancient harbours of Krane, Lechaion/Corinth, Lefkada, Palairos-Pogonia, Pheia/Olympia and others revealed an approximate recurrence interval for mega-tsunamis of approximately 500-1000 years.

7. Acknowledgements

We are indebted to Dipl.-Geol. Peter Henning (Mainz) for carefully proofreading the manuscript. Thanks are due the regional government (Nomarchia) and the diocese of Cefalonia as well as to the 35th Ephorate of Prehistoric and Classical Antiquities for support during fieldwork. Palaeotsunami studies along the eastern shores of the Ionian Seas were funded by the German Research Council (DFG, VO 938/3-1) which is gratefully acknowledged.

9. References

- Ad-hoc-Arbeitsgruppe Boden 2005 – Ad-hoc-Arbeitsgruppe Boden, Bodenkundliche Kartieranleitung, 5th edition (Hannover 2005).
- Ambraseys 2009 – N. Ambraseys, Earthquakes in the Mediterranean and Middle East. A multidisciplinary study of seismicity up to 1900 Cambridge (Cambridge 2009).
- Bernasconi et al. 2006 – M.P. Bernasconi, R. Melis, J.-D. Stanley, Benthic biofacies to interpret Holocene environmental changes and human impact in Alexandria's Easter Harbour, Egypt, *The Holocene* 16/8, 2006, 1163-1176.
- Biedermann 1887 – G. Biedermann, Die Insel Kephallenia im Altertum, Dissertation, Hohe philosophische Fakultät der Universität Würzburg (München 1887).
- Blume et al. 2011 – H.-P. Blume, K. Stahr, P. Leinweber, Bodenkundliches Praktikum. Eine Einführung in pedologisches Arbeiten für Ökologen, insbesondere Land- und Forstwirte, und für Geowissenschaftler, 3rd edition (Heidelberg 2011).
- Bony et al. 2011 – G. Bony, N. Marriner, C. Morhange, D. Kaniewski, D. Perinçek, A high-energy deposit in the Byzantine harbor of Yenikapı, Istanbul (Turkey), *Quaternary International*, 2011, doi:10.1016/j.quaint.2011.03.031.
- Brückner et al. 2006 – H. Brückner, M. Müllenhoff, R. Gehrels, A. Herda, M. Knipping, A. Vött, From archipelago to floodplain – geographical and ecological changes in Miletus and its environs during the past six millennia (Western Anatolia, Turkey), *Zeitschrift f. Geomorphologie N. F., Suppl. Vol. 142*, 2006, 63-83.
- Cavaleri 2005 – L. Cavaleri, The wind and wave atlas of the Mediterranean Sea – the calibration phase, *Advances in Geosciences* 2, 2005, 255-257.
- Clément et al. 2000 – C. Clément, A. Hirn, P. Charvis, M. Sachpazi, F. Marnelis, Seismic structure and the active Hellenic subduction in the Ionian islands, *Tectonophysics*, 329, 2000, 141-156.

- De Martini et al. 2010 – P.M. De Martini, M.S. Barbano, A. Smedile, F. Gerardi, D. Pantosti, P. Del Carlo, C. Pirrotta, A unique 4000 year long geological record of multiple tsunami inundations in the Augusta Bay (eastern Sicily, Italy), *Marine Geology* 276, 2010, 42-57.
- Doutsos and Kokkalas 2001 – T. Doutsos, S. Kokkalas, Stress and deformation patterns in the Aegean region, *Journal of Structural Geology* 23, 2001, 455-472.
- Engel et al. 2009 – M. Engel, M. Knipping, H. Brückner, M. Kiderlen, J.C. Kraft, Reconstructing middle to late Holocene palaeogeographies of the lower Messenian plain (southwestern Peloponnese, Greece): Coastline migration, vegetation history, and sea level change, *Palaeogeography, Palaeoclimatology, Palaeoecology* 284, 2009, 257-270.
- Fouache et al. 2008 – E. Fouache, M. Ghilardi, K. Vouvalidis, G. Syrides, G. Styllas, S. Kunesch, S. Stiros, Contribution on the Holocene Reconstruction of Thessaloniki Coastal Plain, Greece, *Journal of Coastal Research* 24/5, 2008, 1161-1173.
- Gehrke and Wirbelauer 2004 – H.-J. Gehrke, E. Wirbelauer, Akarnania and adjacent areas, in M.H. Hansen, T.H. Nielsen (eds.), *An inventory of Archaic and Classical Poleis*, Oxford, 2004, 351-378.
- Ghilardi et al. 2008 – M. Ghilardi, S. Kunesch, M. Styllas, E. Fouache, Reconstruction of mid-Holocene sedimentary environments in the central part of the Thessaloniki plain (Greece), based on microfaunal identification, magnetic susceptibility and grain-size analyses, *Geomorphology* 97, 2008, 617-630.
- Giraudi 2009 – C. Giraudi, Late Holocene Evolution of Tiber River Delta and Geoarchaeology of Claudius and Trajan Harbor, Rome, *Geoarchaeology: An International Journal* 24/3, 2009, 371-382.
- Goiran 2010 – J.-P. Goiran, Palaeoenvironmental reconstruction of the ancient harbors of Rome: Claudius and Trajan's marine harbors on the Tiber delta, *Quaternary International* 216, 2010, 3-13.
- Goiran et al. 2011 – J.P. Goiran, K.P. Pavlopoulos, E. Fouache, M. Triantaphyllou, R. Etienne, Piraeus, the ancient island of Athens: Evidence from Holocene sediments and historical archives, *Geology* 39/6, 2011, 531-534.
- Goodman-Tchernov et al. 2009 – B. Goodman-Tchernov, H.W. Dey, E.G. Reinhardt, F. McCoy, Y. Mart, Tsunami waves generated by the Santorini eruption reached eastern Mediterranean shores, *Geology* 37/10, 2009, 943-946.
- Guidoboni and Comastri 2005 – E. Guidoboni, A. Comastri, Catalogue of earthquakes and tsunamis in the Mediterranean area from the 11th to the 15th century, Volume 2, INGV-SGA (Bologna 2005).
- Hadler et al. 2011 – H. Hadler, A. Vött, B. Koster, M. Mathes-Schmidt, T. Mattern, K. Ntageretzis, K. Reicherter, D. Sakellariou, T. Willershäuser, Lechaion, the ancient harbour of Corinth (Peloponnese, Greece) destroyed by tsunamigenic impact, in C. Grützner, R. Pérez-Lopez, T. Fernández Steeger, I. Papanikolaou, K. Reicherter, P.G. Silva, A. Vött (eds.), *Earthquake Geology and Archaeology: Science, Society and Critical facilities. Proceedings of the 2nd INQUA-IGCP 567 International Workshop on Active Tectonics, Earthquake Geology, Archaeology and Engineering, 19-24 September 2011, Corinth (Greece), Corinth, 2011, 70-73.*
- Haslinger et al. 1999 – F. Haslinger, E. Kissling, J. Ansorge, D. Hatzfeld, E. Papadimitriou, V. Karakostas, K. Makropoulos, H.-G. Kahle, Y. Peter, 3D crustal structure from local earthquake tomography around the Gulf of Arta (Ionian region, NW Greece), *Tectonophysics* 304, 1999, 201-218.
- Hofrichter 2002 – R. Hofrichter (ed.), *Das Mittelmeer. Fauna, Flora, Ökologie. Band I: Allgemeiner Teil* (Heidelberg/Berlin 2002).

- Hollenstein et al. 2008a – C. Hollenstein, M.D. Müller, A. Geiger, H.-G. Kahle, Crustal motion and deformation in Greece from a decade of GPS measurements, 1993-2003, *Tectonophysics* 449, 2008, 17-40.
- Hollenstein et al. 2008b – C. Hollenstein, M.D. Müller, A. Geiger, H.-G. Kahle, GPS-derived coseismic displacements associated with the 2001 Skyros and 2003 Lefkada earthquakes in Greece, *Bulletin of the Seismological Society of America* 98/1, 2008, 149-161.
- IGME 1985 – Institute of Geology and Mineral Exploration (IGME), Geological map of Greece, 1:50,000, Cephalonia Island (southern part) (Athens 1985).
- Kortekaas et al. 2011 – S. Kortekaas, G.A. Papadopoulos, A. Ganas, A.B. Cundy, A. Diakantoni, Geological identification of historical tsunamis in the Gulf of Corinth, Central Greece, *Natural hazards and Earth System Sciences* 11, 2011, 2029-2041.
- Lagios et al. 2007 – E. Lagios, V. Sakkas, P. Papadimitriou, I. Parcharidis, B.N. Damiata, K. Chousianitis, S. Vassilopoulou, Crustal deformation in the Central Ionian Islands (Greece): Results from DGPS and DInSAR analyses (1995-2006), *Tectonophysics* 444, 2007, 119-145.
- Marriner and Morhange 2007 – N. Marriner, C. Morhange, *Geoscience of ancient Mediterranean harbours*, *Earth-Science Reviews* 80, 2007, 137-194.
- Marriner et al. 2010 – N. Marriner, C. Morhange, J.P. Goiran, Coastal and ancient harbour geoarchaeology, *Geology Today* 26/1, 2010, 21-27.
- May et al. 2011 – S.M. May, A. Vött, H. Brückner, R. Grapmayer, M. Handl, V. Wennrich, The Lefkada barrier and beachrock system (NW Greece) – controls on coastal evolution and the significance of extreme wave events, *Geomorphology*, 2011, <http://dx.doi.org/10.1016/j.geomorph.2011.10.038>
- Medatlas Group 2004 – The Medatlas Group, Wind and wave atlas of the Mediterranean Sea, Western European Union, WEAO Research Cell, 2004.
- Morhange and Marriner 2010 – C. Morhange, N. Marriner, Paleo-hazards in the coastal Mediterranean: a geoarchaeological approach, in I.P. Martini, W. Chesworth (eds.), *Landscapes and societies. Selected cases*, Dordrecht/Heidelberg/London/New York, 2010, pp. 223-234.
- Moschopoulos and Marabegia-Kosta 2007 – G.N. Moschopoulos, K. Marabegia-Kosta, *The Argostoli Earthquake 1953. Beginning and end of a town*, 2th edition (Argostoli 2007).
- Müllenhoff 2005 – M. Müllenhoff, *Geoarchäologische, sedimentologische und morphodynamische Untersuchungen im Mündungsgebiet des Büyük Menderes (Mäander)*, Westtürkei, *Marburger Geographische Schriften* 141 (Marburg/Lahn 2005).
- Orama Editions (2011) – Orama Editions, Road and Tourist Map, Cephalonia/Ithaka, scale 1:75000. 7th edition (Rafina 2011).
- Papadimitriou et al. 2006 – P. Papadimitriou, G. Kaviris, K. Makropoulos, The Mw = 6.3 2003 Lefkada earthquake (Greece) and induced stress transfer changes, *Tectonophysics* 423, 2006, 73-82.
- Papazachos and Dimitriu 1991 – B.C. Papazachos, P.P. Dimitriu, Tsunamis in and near Greece and their relation to the earthquake focal mechanism, in E.N. Bernard (ed.), *Tsunami hazard. A practical guide for tsunami hazard reduction*, *Natural Hazards* 4/2-3, 1991, 161-170.
- Partsch 1890 – J. Partsch, *Kephallenia und Ithaka. Eine geographische Monographie*. Petermanns Geographische Mitteilungen, *Ergänzungsheft* 98 (Gotha 1890).
- Poppe and Goto 1991 – G.T. Poppe, Y. Goto, *European seashells. Volume I: Polyplacophora, Caudofoveata, Solenogastra, Gastropoda*. ConchBooks (Wiesbaden 1991).

- Poppe and Goto 2000 – G.T. Poppe, Y. Goto, European seashells. Volume II: Scaphopoda, Bivalvia, Cephalopoda (Hackenheim 2000).
- Reimer and McCormac 2002 – P.J. Reimer, F.G. McCormac, Marine radiocarbon reservoir corrections for the Mediterranean and Aegean Seas, *Radiocarbon* 44, 2002, 159-166.
- Reimer et al. 2009 – P.J. Reimer, M.G.L. Baillie, E. Bard, A. Bayliss, J.W. Beck, P.G. Blackwell, C. Bronk Ramsey, C.E. Buck, G.S. Burr, R.L. Edwards, M. Friedrich, P.M. Grootes, T.P. Guilderson, I. Hajdas, T.J. Heaton, A.G. Hogg, K.A. Hughen, K.F. Kaiser, B. Kromer, F.G. McCormac, S.W. Manning, R.W. Reimer, D.A. Richards, J.R. Southon, S. Talamo, C.S.M. Turney, J. van der Plicht, C.E. Weyhenmeyer, *IntCal09 and Marine09 radiocarbon age calibration curves, 0-50,000 years cal BP*, *Radiocarbon* 51, 2009, 1111-1150.
- Reinhardt et al. 2006 – E.G. Reinhardt, B.N. Goodman, J.I. Boyce, G. Lopez, P. van Henstum, W.J. Rink, Y. Mart, A. Raban, The tsunami of 13 December A.D. 115 and the destruction of Herod the Great's harbor at Caesarea Maritima, Israel, *Geology* 34/12, 2006, 1061-1064.
- Sachpazi et al. 2000 – M. Sachpazi, A. Hirn, C. Clément, F. Haslinger, M. Laigle, E. Kissling, P. Charvis, Y. Hello, J.-C. Lépine, M. Sapin, J. Ansorge, Western Hellenic subduction and Cephalonia Transform: local earthquakes and plate transport and strain, *Tectonophysics* 319/4, 2000, 301-319.
- Scheffers et al. 2008 – A. Scheffers, D. Kelletat, A. Vött, S.M. May, S. Scheffers, Late Holocene tsunami traces on the western and southern coastlines of the Peloponnesus (Greece), *Earth Planetary Science Letters* 269, 2008, 271-279.
- Scicchitano et al. 2007 – G. Scicchitano, C. Monaco, L. Tortorici, Large boulder deposits by tsunami waves along the Ionian coast of south-eastern Sicily (Italy), *Marine Geology* 238, 2007, 75-91.
- Scicchitano et al. 2010 – G. Scicchitano, B. Costa, A. Di Stefano, S.G. Longhitano, C. Monaco, Tsunami and storm deposits preserved within a ria-type rocky coastal setting (Siracusa, SE Sicily), *Zeitschrift f. Geomorphologie N.F., Suppl. Issue 54/3*, 2010, 51-77.
- Scordilis et al. 1985 – E. Scordilis, G. Karakaisis, D. Panagiotopoulos, B. Papazachos, Evidence for transform faulting in the Ionian Sea: the Cephalonia Island earthquake sequence of 1983, *Pageoph* 123, 1985, 387-397.
- Smedile et al. 2011 – A. Smedile, P.M. De Martini, D. Pantosti, L. Bellucci, P. Del Carlo, L. Gasperini, C. Pirrotta, A. Polonia, E. Boschi, Possible tsunami signatures from an integrated study in the Augusta Bay offshore (Eastern Sicily – Italy), *Marine Geology* 281, 2011, 1-13.
- Soukissian et al. 2007 – T. Soukissian, M. Hatzinaki, G. Korres, A. Papadopoulos, G. Kallos, E. Anadranistakis, *Wind and wave atlas of the Hellenic Seas*, Hellenic Center for Marine Research Publications (Athens 2007).
- Soukissian et al. 2008 – T. Soukissian, A. Prospathopoulos, M. Hatzinaki, M. Kabouridou, Assessment of the wind and wave climate of the Hellenic seas using 10-year hindcast results, *The Open Ocean Engineering Journal* 1, 2008, 1-12.
- Stanley and Bernasconi 2006 – J.-D. Stanley, M.P. Bernasconi, Holocene depositional patterns and evolution in Alexandria's eastern harbor, Egypt, *Journal of Coastal Research* 22/2, 2006, 283-297.
- Stiros et al. 1994 – S.C. Stiros, M. Arnold, P.A. Pirazzoli, J. Laborel, F. Laborel-Deguen, The 1953 earthquake in Cephalonia (western Hellenic arc): Coastal uplift and halotectonic faulting, *Geophysical Journal International* 117, 1994, 834-849.

- Tsimplis and Shaw 2010 – M.N. Tsimplis, A.G.P. Shaw, Seasonal sea level extremes in the Mediterranean Sea and at the Atlantic European coasts, *Natural Hazards of Earth System Sciences* 10, 2010, 1457-1475.
- Vött 2007 – A. Vött, Silting up Oiniadai's harbours (Acheloos River delta, NW Greece) – geoarchaeological implications of late Holocene landscape changes, *Géomorphologie: relief, processus, environnement* 1, 2007, 19-36.
- Vött and Brückner 2006 – A. Vött, H. Brückner, Versunkene Häfen im Mittelmeerraum. Antike Küstenstädte als Archive für die Kultur- und Umweltforschung, *Geographische Rundschau* 58/4, 2006, 12-21.
- Vött et al. 2006 – A. Vött, M. May, H. Brückner, S. Brockmüller, Sedimentary evidence of late Holocene tsunami events near Lefkada Island (NW Greece), *Zeitschrift f. Geomorphologie N.F., Suppl. Vol. 146*, 2006, 139-172.
- Vött et al. 2007 – A. Vött, A. Schriever, M. Handl, H. Brückner, Holocene palaeogeographies of the central Acheloos River delta (NW Greece) in the vicinity of the ancient seaport Oiniadai, *Geodinamica Acta* 20/4, 2007, 241-256.
- Vött et al. 2009a – A. Vött, H. Brückner, S. Brockmüller, M. Handl, S.M. May, K. Gaki-Papanastassiou, R. Herd, F. Lang, H. Maroukian, O. Nelle, D. Papanastassiou, Traces of Holocene tsunamis across the Sound of Lefkada, NW Greece, *Global and Planetary Change* 66, 2009, 112-128.
- Vött et al. 2009b – A. Vött, H. Brückner, S.M. May, D. Sakellariou, O. Nelle, F. Lang, V. Kapsimalis, S. Jahns, R. Herd, M. Handl, I. Fountoulis, The Lake Voulkaria (Akarnania, NW Greece) palaeoenvironmental archive – a sediment trap for multiple tsunami impact since the mid-Holocene, *Zeitschrift f. Geomorphologie N.F., Suppl. Issue 53/1*, 2009, 1-37.
- Vött et al. 2010 – A. Vött, G. Bareth, H. Brückner, C. Curdt, I. Fountoulis, R. Grapmayer, H. Hadler, D. Hoffmeister, N. Klasen, F. Lang, P. Masberg, S.M. May, K. Ntageretzis, D. Sakellariou, T. Willershäuser, Beachrock-type calcarenitic tsunamites along the shores of the eastern Ionian Sea (western Greece) – case studies from Akarnania, the Ionian Islands and the western Peloponnese, *Zeitschrift f. Geomorphologie N.F., Suppl. Issue 54/3*, 2010, 1-50.
- Vött et al. 2011a – A. Vött, F. Lang, H. Brückner, K. Gaki-Papanastassiou, H. Maroukian, D. Papanastassiou, A. Giannikos, H. Hadler, M. Handl, K. Ntageretzis, T. Willershäuser, A. Zander, Sedimentological and geoarchaeological evidence of multiple tsunamigenic imprint on the Bay of Palairos-Pogonia (Akarnania, NW Greece), *Quaternary International* 242, 2010, 213-239.
- Vött et al. 2011b – A. Vött, G. Bareth, H. Brückner, F. Lang, D. Sakellariou, H. Hadler, K. Ntageretzis, T. Willershäuser, Olympia's harbour site Pheia (Elis, western Peloponnese, Greece) destroyed by tsunami impact, *Die Erde* 142/3, 259-288.
- Warnecke 2008 – H. Warnecke, Homers Wilder Westen. Die historisch-geographische Wiedergeburt der Odyssee (Stuttgart 2008).
- Willershäuser et al. 2011 – T. Willershäuser, A. Vött, H. Brückner, G. Bareth, H. Hadler, K. Ntageretzis, New insights in the Holocene evolution of the Livadi coastal plain, Gulf of Argostoli (Cefalonia, Greece), in V. Karius, H. Hadler, M. Deicke, H. von Eynatten, H. Brückner, A. Vött (eds.), *Dynamische Küsten – Grundlagen, Zusammenhänge und Auswirkungen im Spiegel angewandter Küstenforschung*, *Coastline Reports* 17, 2011, 99-110, <http://www.eucc-d.de/coastline-reports-17-2011.html>.
- Zhu and Weindorf 2010 – Y. Zhu, D. Weindorf, Determination of soil calcium using field portable X-ray fluorescence, *Soil Science* 174/3, 2010, 151-155.

Figure captions

Fig. 1: Detail map of the Bay of Koutavos and the Koutavos coastal plain in the environs of ancient Krane. White dots mark vibracoring sites. Earth resistivity measurements were carried out along the shore near site KOU 1A, marked by thin white lines. Map based on Topographic Map 1:75,000 Cephalonia/Ithaka (Orama Editions 2011) and Google Earth images (2005).

Fig. 2: Overview of the southern part of the Gulf of Argostoli showing the SE-NW trending cul-de-sac-type annex formed by the Bays of Argostoli and Koutavos. Note that water depths in the gulf are much deeper (> 20 m) than in the inner Bay of Argostoli (< 10 m) and in the Bay of Koutavos (< 1 m). The Bays of Argostoli and Koutavos represent an excellent natural harbour setting completely sheltered from storm influence. Bathymetric data after Orama Editions (2011), map based on Google Earth images (2009).

Fig. 3: Geographical and tectonic overview of the Ionian and Aegean Seas. (a) Cefalonia Island exposed to the seismically highly active Hellenic Arc where subduction, transform faulting and collision between different plates is taking place (after Haslinger et al. 1999, Doutsos and Kokkalas 2001). (b) Local fault systems on Cefalonia Island after Stiros et al. (1994) and IGME (1985). Note the Argostoli Fault which is responsible for the fact that the Bay of Koutavos forms a cul-de-sac-type annex to the Gulf of Argostoli. (c) Tsunamigenic sources in Greece after Papazachos and Dimitriu (1991), known and inferred from tsunami catalogues. Ellipse size is proportional to the (estimated) maximum tsunami intensity.

Fig. 4: Bird's eye view towards the NW of the Koutavos coastal plain, the Bays of Koutavos and Argostoli and the Gulf of Argostoli. In the background, the Bay of Livadi marks the northern end of the gulf. Vibracoring sites are marked with white ellipsoidal dots. Note the Argostoli Promontory with Cape Aghios Theodoron at its northwestern end which separates the Koutavos annex from the gulf. Figure based on Google Earth image (2009).

Fig. 5: (a) Simplified facies distribution pattern for vibracore KRA 7 drilled in the central Koutavos coastal plain. Note the coarse-grained high-energy tsunami deposits out of allochthonous sand, gravel and shell debris intersecting autochthonous fine-grained silty sediments. (b) Youngest tsunami layer out of sand and marine shell fragments with sharp erosional unconformity at the base. (c) Youngest but one tsunamite encountered at site KRA 7

showing basal erosional unconformity, layering and clayey to silty rip-up clasts out of lagoonal deposits incorporated into the high-energy deposit.

Fig. 6: Transect of vibracores KRA 1 to 4, 6 and 7 drilled in the Koutavos coastal plain. For location of vibracoring sites see Fig. 1.

Fig. 7: Simplified facies distribution pattern for vibracore KRA 8 drilled at the southern shore of the Bay of Koutavos. The tsunamigenic interference between approximately 1.50-2.00 m b.s., made out of sand and shell debris, differs considerably from the autochthonous silt-dominated distal alluvial fan sediments.

Fig. 8: Simplified facies distribution pattern for vibracore KRA 9 drilled at the eastern shore of the Bay of Koutavos. Tsunami influence is depicted in the form of multiple layers out of coarse-grained sediments and marine shell debris intersecting homogeneous lagoonal deposits. The uppermost part of the profile consists of building rubble dumped at the site after the catastrophic earthquake that destroyed large parts of Argostoli city in 1953.

Fig. 9: Transect of vibracores KRA 5, 8 and 9 drilled along the shore of the Bay of Koutavos and vibracore KRA 7 from the western Koutavos coastal plain. For location of vibracoring sites see Fig. 1, for legend see Fig. 6.

Fig. 10: Simplified results from earth resistivity measurements along transects KOU ERT 1 and KOU ERT 2 conducted at the shore of the Bay of Koutavos near vibracoring site KOU 1A. For location of transects see Fig. 1, for further explanations see text.

Fig. 11: Ca/Ti ratios for vibracores drilled in the Koutavos coastal plain and at the shores of the Bay of Koutavos based on XRF measurements. Ca/Ti peaks indicate non-equilibrium temporary interferences of the ecological system by high-energy impact from the sea side. For location of vibracoring sites see Fig. x; for further explanation see text.

Fig. 12: Tsunami landfall scenario for the Gulf of Argostoli and the Bays of Argostoli and Koutavos based on a northward propagating tsunami event generated in the environs of the Hellenic Arc. (a) Topographic overview showing the funnel-type coastal configuration at the entrance of the Gulf of Argostoli. (b) to (d) Tsunami wave propagation and tsunami landfall

in the Kootavos coastal plain due to wave amplification, acceleration, refraction, diffraction and reflection. Maps based on Topographic Map 1:75,000 (Orama Editions 2011) and Google Earth images (2009). See text for further explanation.

Table 1: Radiocarbon dates of samples from vibracores drilled in the environs of ancient Krane (Cefalonia Island).

Note: b.s. – below ground surface; b.s.l. – below sea level; 1σ max; min cal BP/BC (AD) – calibrated ages, 1σ -range; “;” – semicolon is used in case there are several possible age intervals due to multiple intersections with the calibration curve; Lab. No. – laboratory number, Leibniz-Laboratory for Radiometric Dating and Isotope Research, Christian-Albrechts-Universität zu Kiel (Kia); * – marine reservoir correction with assumed mean reservoir age of 402 years. Calibration based on Calib 6.0 software (Reimer et al. 2009).

Figure 1

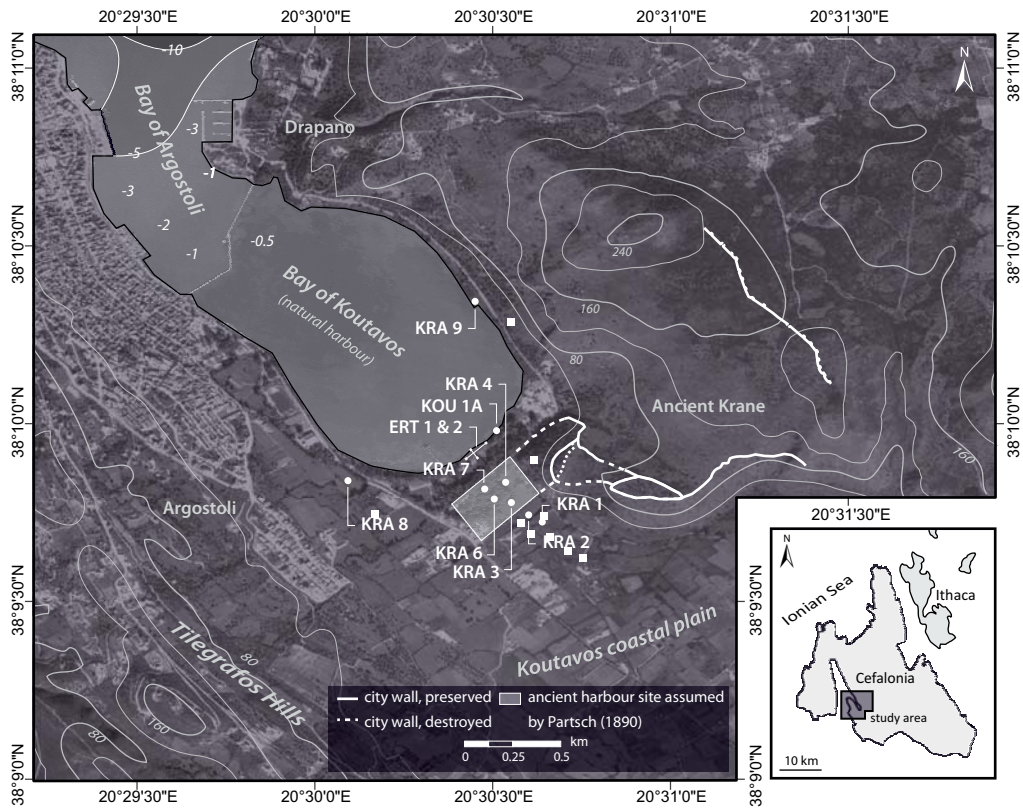


Figure 2

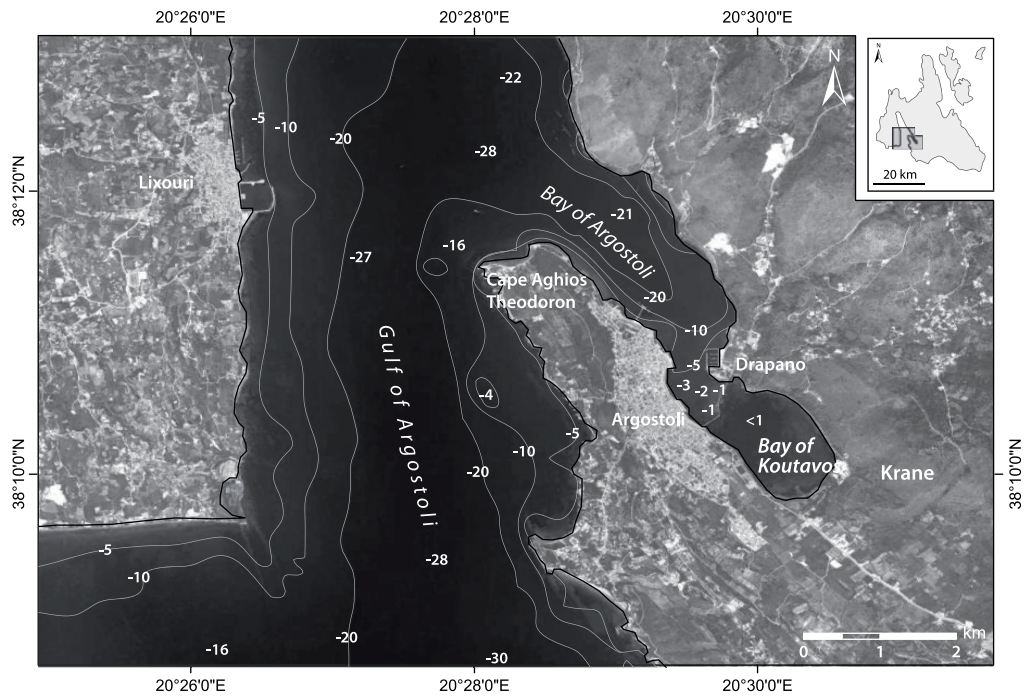


Figure 3

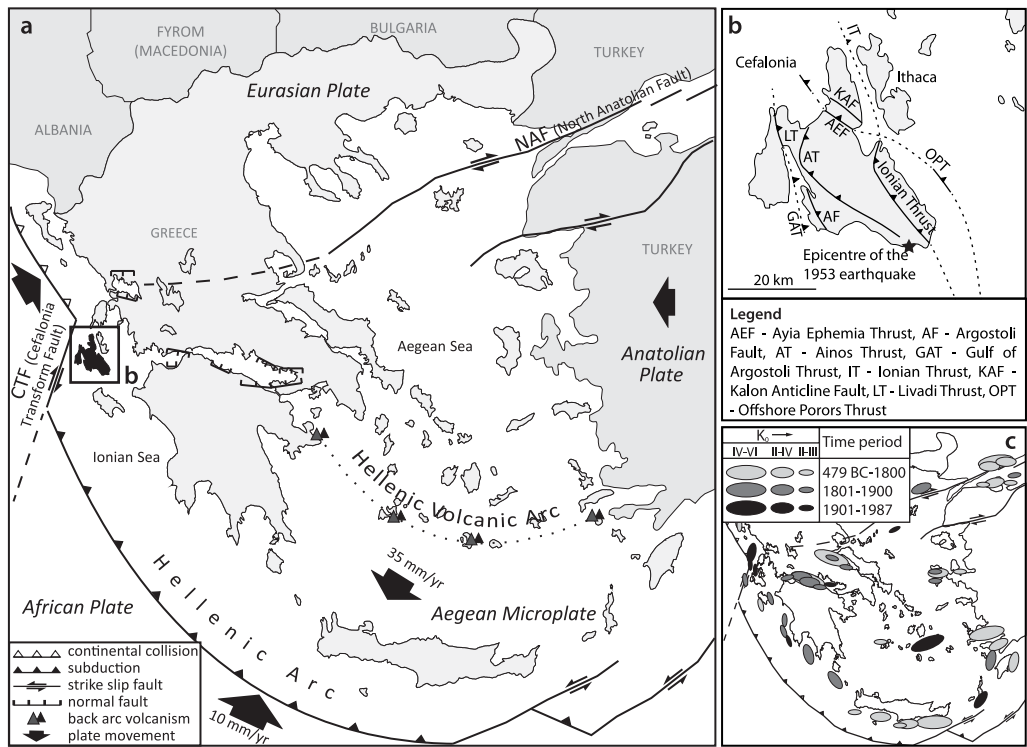


Figure 4

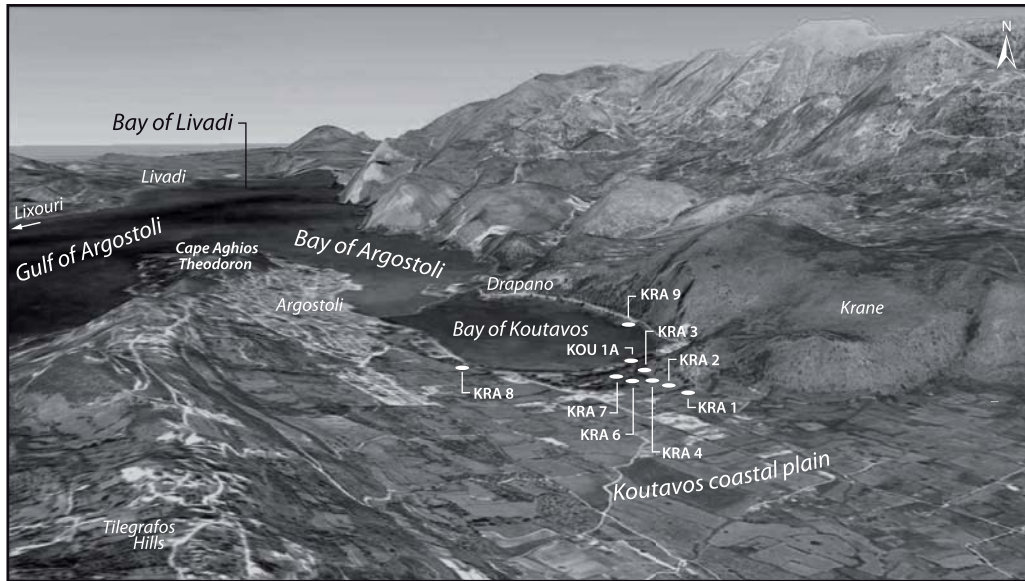


Figure 5

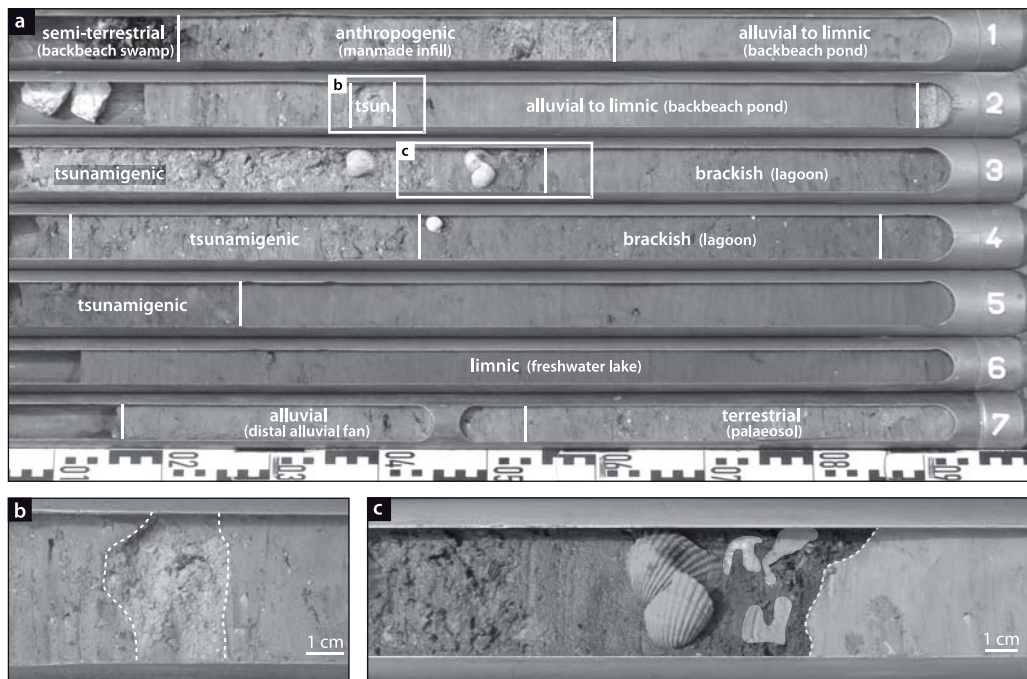


Figure 6

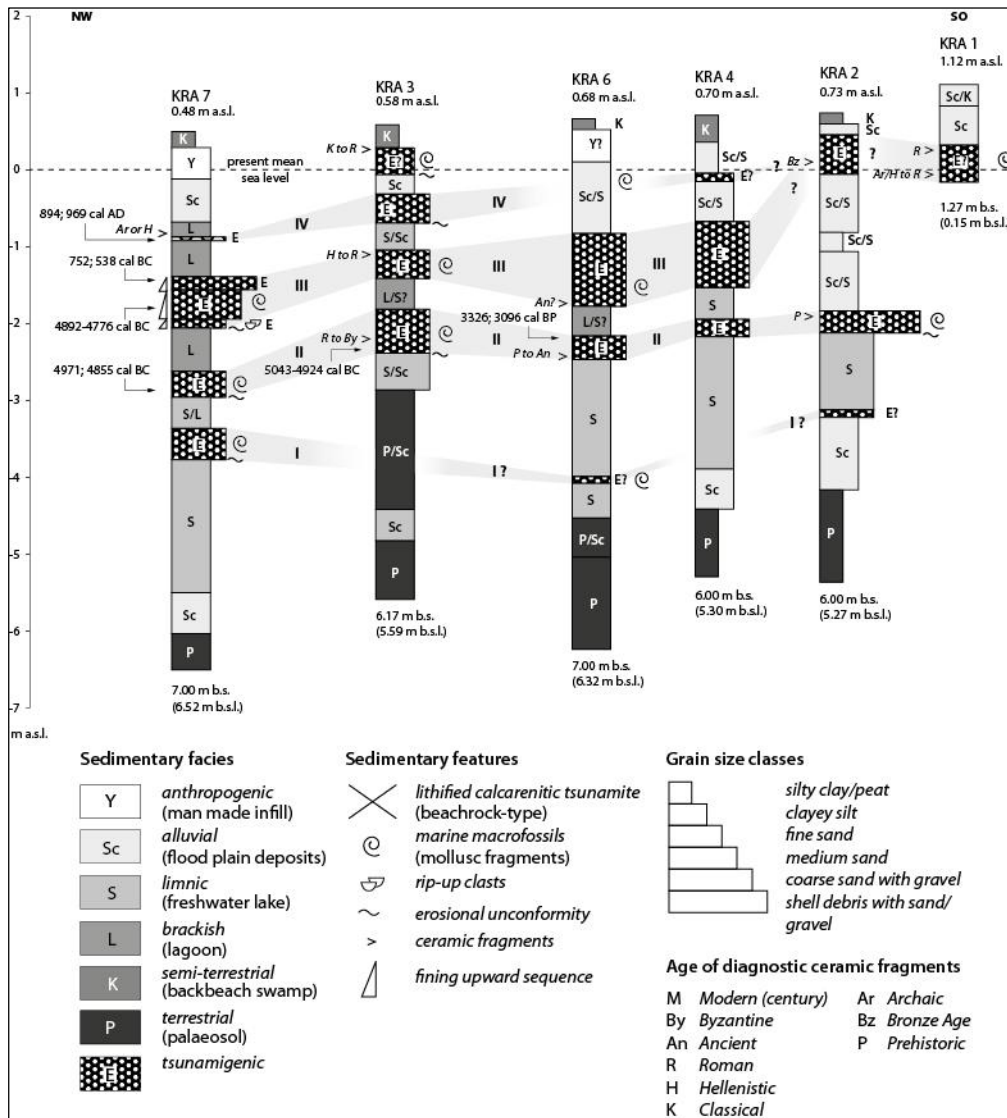


Figure 7

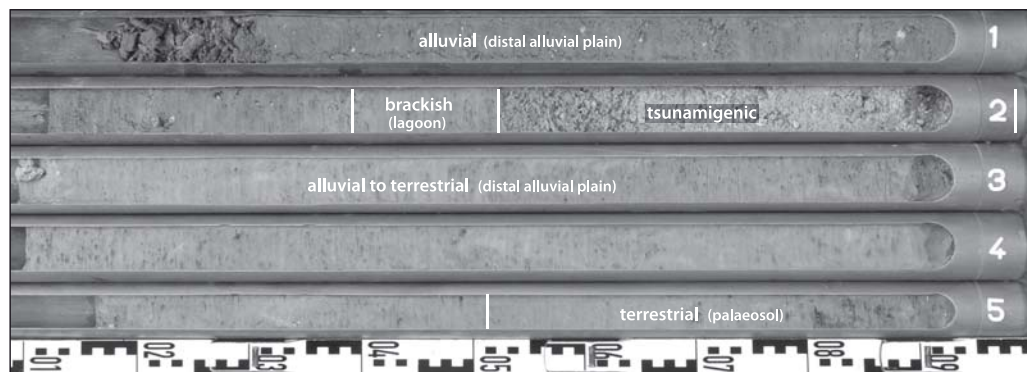


Figure 8

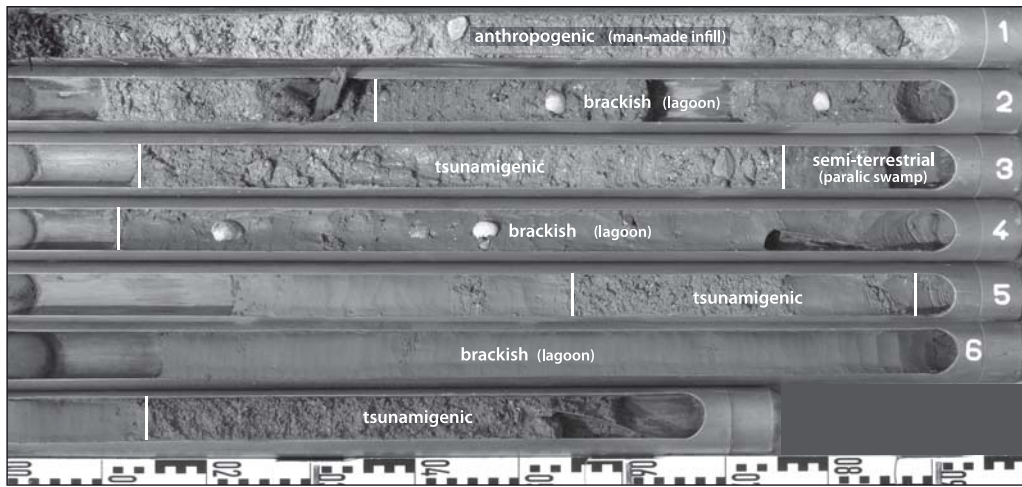


Figure 9

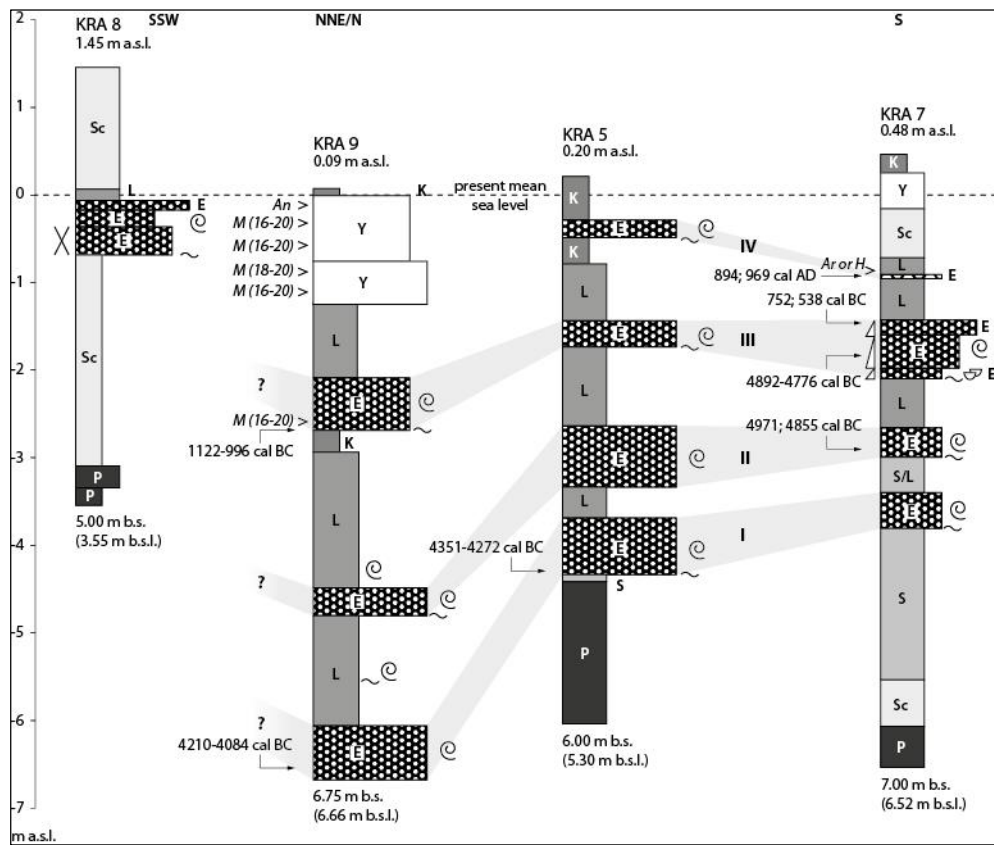


Figure 10

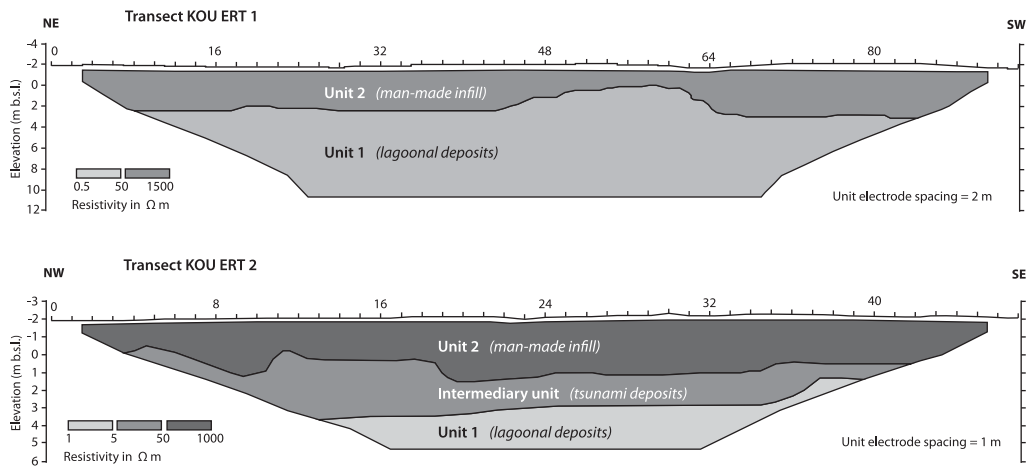


Figure 11

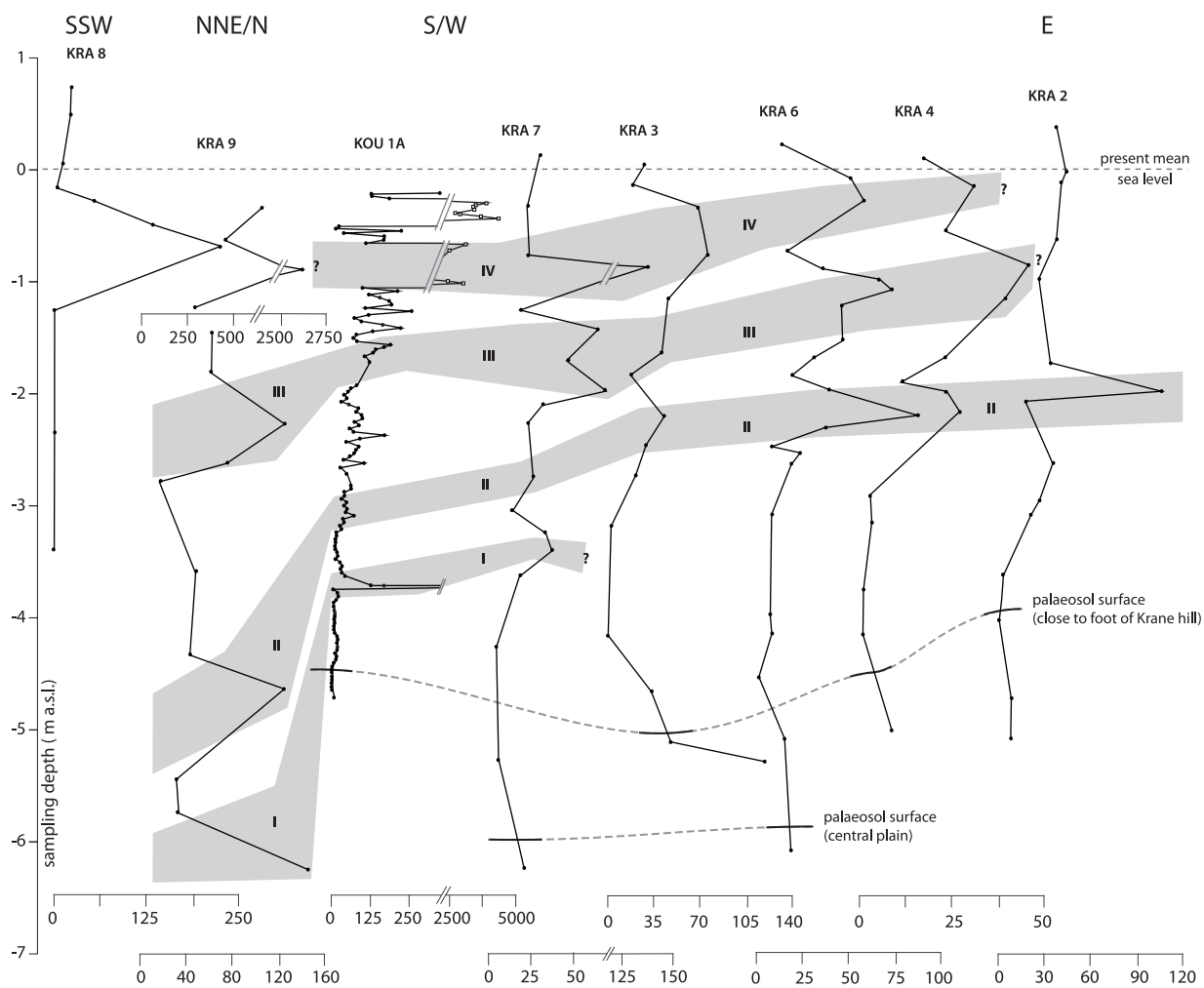
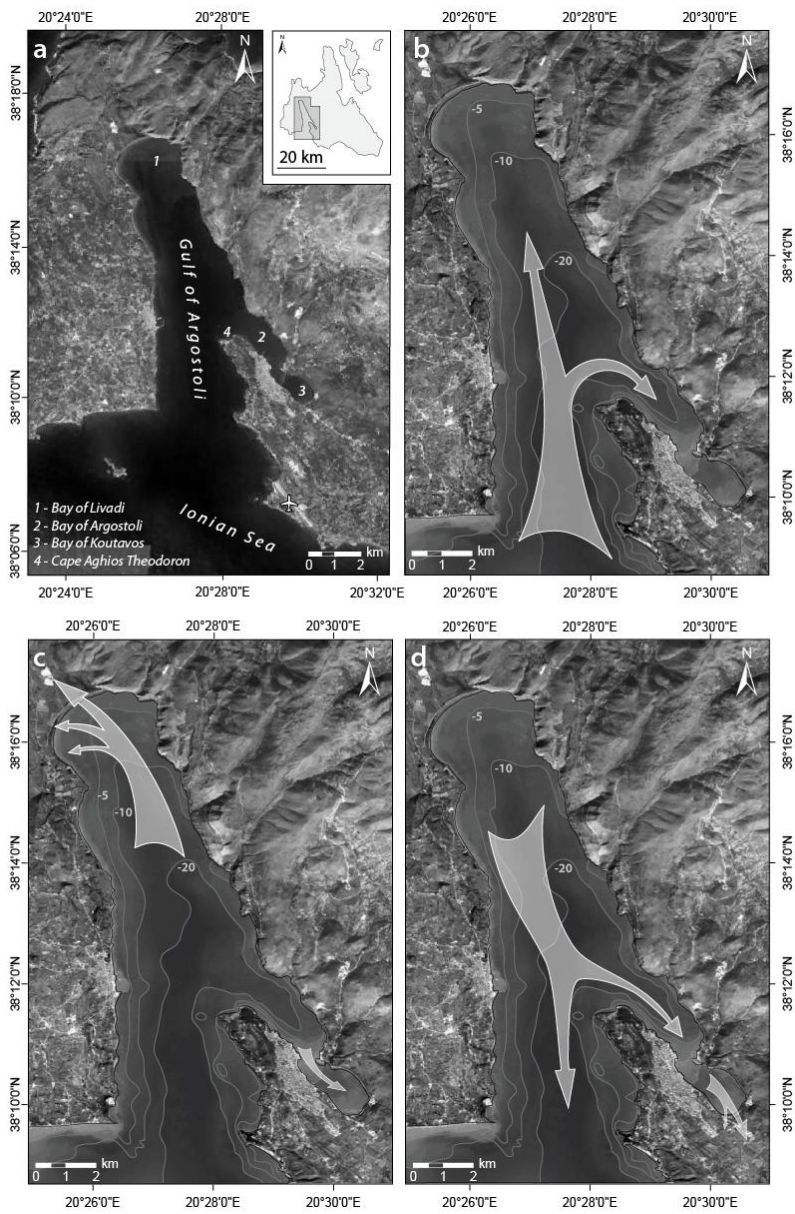


Figure 12



Sample Name	Depth (m b.s.)	Depth (m b.s.l.)	Sample Description	Lab. No. (Kia)	$\delta^{13}\text{C}$ (ppm)	^{14}C Age (BP)	1 σ max; min (cal BP)	1 σ max; min (cal BC)
KRA 3/9 M	2.85	0.76	<i>Scrobicularia</i> sp., articulated specimen	39692	-0.40 \pm 0.34	6445 \pm 40	6992 – 6873	5043 – 4924*
KRA 5/9+ M	4.16	3.96	<i>Dosinia exoleta</i> , articulated specimen	39693	1.80 \pm 0.45	5850 \pm 35	6300 – 6221	4351 – 4272*
KRA 6/13 HK	2.86	2.18	charcoal	39694	-23.70 \pm 0.34	4475 \pm 25	5275; 5045	3326; 3096
KRA 7/4 HK	1.41	0.93	charcoal	39695	-26.70 \pm 0.13	1120 \pm 25	1056; 981	894 AD; 969 AD
KRA 7/6 HK	1.90	1.42	charcoal	39696	-24.87 \pm 0.15	2475 \pm 25	2701; 2487	752; 538
KRA 7/7 M	2.26	1.78	<i>Cerastoderma glaucum</i> , articulated specimen	39698	-5.38 \pm 0.34	6320 \pm 40	6841 – 6725	4892 – 4776*
KRA 7/11+ M	3.25	2.77	<i>Scrobicularia</i> sp., articulated specimen	39699	-5.01 \pm 0.36	6390 \pm 35	6920; 6804	4971; 4855*
KRA 9/8+ M	2.75	2.66	<i>Dosinia exoleta</i> , articulated specimen	39700	-4.86 \pm 0.22	3205 \pm 35	3071 – 2945	1122 – 996*
KRA 9/15+ M	6.49	6.29	<i>Loripes lacteus</i> , single valve	39701	0.29 \pm 0.15	5680 \pm 35	6159 – 6033	4210 – 4084*

Table 1